

Integrated High-Precision Measurement of Multi-Freeform Surface Prisms

Chen Li¹, Shibin Xiao¹, Changshuai Fang¹, Zexiao Li¹ and Xiaodong Zhang^{1,#}

¹ State Key Laboratory of Precision Measuring Technology & Instruments, Laboratory of Micronano Manufacturing Technology, Tianjin University, Tianjin 300072, China

Corresponding Author / Email: Zhangxd@tju.edu.cn

KEYWORDS: Integrated measurement, Freeform prism, Automated correction of measurement path, Multi-axis measurement system

With the advancement of manufacturing technology and the increasing application demands, optical systems are being developed towards miniaturization and high optical performance. As a crucial means to meet these demands, optical freeform surfaces offer high design flexibility, allowing the surface shape to be adjusted according to imaging requirements and overcoming the limitations of traditional spherical and aspherical designs. The introduction of freeform elements can significantly reduce the number of components in an optical system. Optical freeform prisms, as typical freeform elements, not only possess image quality control capabilities but also enable optical path folding, thereby reducing the size of the optical system. The optical performance of freeform prisms is influenced by the precision of each surface and the relative positions between surfaces. Therefore, when such devices are measured, it is essential for all surfaces to be comprehensively sampled in a single measurement process. High rotational degrees of freedom are required for the measurement system, and accurate measurement paths must be designed according to the sensor's angular characteristics. Current optical element measurement equipment can measure only a single surface. To address this, a five-axis line-scan system has been developed, and an iterative measurement algorithm has been proposed that can automatically correct the measurement path, ultimately achieving comprehensive measurement of optical freeform prisms.

1. Introduction

Polyhedral freeform surface prisms can achieve complex optical functions, providing a new approach to the design and selection of optical systems due to their unique spatial structure and optical properties. In recent years, with the continuous improvement of optical design capabilities, the application of freeform surface prisms has gradually increased, playing a special role in various fields. Freeform surface prisms can fold the optical path in complex optical systems such as HMD (head-mounted display) systems, periscope systems, and infrared imaging systems, ensuring imaging performance while reducing system volume and improving system stability [1][2]. The morphology of each surface and the relative relationship between each surface of a polyhedral freeform prism significantly impact its optical performance. In industrial sites, it is necessary to efficiently measure all areas of its surface to ensure that the measurement results include both the quality information of a single surface and the quality information of the relative relationship between each surface, facilitating a complete evaluation of its processing quality. Investigation indicates a lack of studies on the integrated measurement of multi-surface prisms.

The line laser measurement method is widely used in the full-profile measurement of parts due to its simple system structure and

calibration method, large field of view and measurement range, fast response speed, and low cost [3]. However, for prisms with directional diffuse reflection on the surface [4], the rationality of the view angle directly affects the S/N of the light stripe. Reducing the permissible range of view angle can lead to an increased demand for path accuracy. Furthermore, the presence of error sources, such as system assembly accuracy and fixture accuracy, affects the precision of path planning. In severe cases, this can result in poor S/N of measurement results, rendering it impossible to complete full-profile measurements. To solve the problem of angle selection in line laser measurement prisms and the contradiction between high path accuracy requirements and the objective existence of error sources, this paper mainly carried out the following work:

Firstly, a scanning measurement system was developed based on a line laser and five axes. Secondly, a method for selecting the optimal view angle of the test surface was introduced, accompanied by a calculation method for S/N of the light stripe. This method ensures the system obtains stable, high-quality light stripe images during the scanning measurement process. Lastly, an iterative measurement method was proposed based on measurement results and model data, which can automatically achieve high-precision full-profile measurement of freeform triangular prisms.

2. Measurement system structure and method.

2.1 Five-axis line laser scanning system structure

To meet the requirements of measuring the full profile of freeform surface prisms, the system must have sufficient degrees of motion, especially rotational degrees of freedom. A motion system consisting of three displacement axes and a cradle mechanism is constructed in this paper, as shown in Figure 1. The cradle mechanism comprises the C-axis and A-axis, which are installed on the cradle mechanism on the horizontal displacement platform composed of the X-axis and Z-axis. The object is fixed on the C-axis. A line laser sensor is installed on the Z-axis. A world coordinate $O_W\text{-}X_WY_WZ_W$ is established based on the position of the sensor. Assuming that the measurement coordinate system of the sensor is $O\text{-}UV$, the origin of the world coordinate system O_W coincides with the origin of the measurement coordinate system O , Z_W , and Y_W , representing the $-U$ and V directions of the measurement coordinate system. X_W and Y_WZ_W form a right-hand coordinate system.

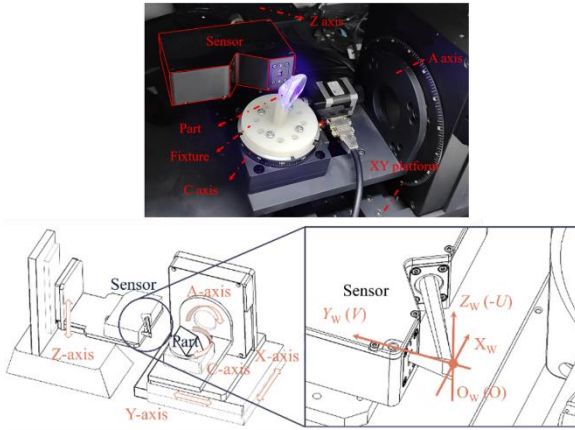


Fig. 1 System structure and world coordinate system.

A world coordinate system based on the measurement coordinate system of the sensor is established in this paper, the coordinate transformation formulas can be subsequently derived as follows: Suppose the positive motion directions of X-axis, Y-axis and Z-axis are $V_x=(v_{xx}, v_{xy}, v_{xz})^T$, $V_y=(v_{yx}, v_{yy}, v_{yz})^T$ and $V_z=(v_{zx}, v_{zy}, v_{zz})^T$. The points on the A-axis and C-axis and their corresponding unit vectors are respectively: $P_{VA}=(x_{VA}, y_{VA}, z_{VA})^T$, $P_{VC}=(x_{VC}, y_{VC}, z_{VC})^T$, $V_{VA}=(v_{VAX}, v_{VAY}, v_{VAZ})^T$ and $V_{VC}=(v_{VCX}, v_{VCY}, v_{VCZ})^T$. After the linear axis has moved $\Delta T=(\Delta x, \Delta y, -\Delta z)^T$ and the A and C rotation axes have moved by angles α_A and α_C , respectively, the coordinates of a point (u, v) in the measurement coordinate system of the line laser sensor can be transformed to the world coordinate system (x, y, z) using the following equations.

$$\begin{bmatrix} 0 \\ v \\ -u \\ 1 \end{bmatrix} = RT_A \cdot RT_C \cdot \begin{bmatrix} x \\ y \\ z \\ 1 \end{bmatrix} + \begin{bmatrix} M_{\Delta} \Delta T \\ 0 \\ 0 \\ 1 \end{bmatrix} \quad (1)$$

Where M_{Δ} is the transformation matrix that converts the motion quantities to the world coordinate system coordinates. RT_A and RT_C are the rotation matrices around the A-axis and C-axis, respectively.

2.2 Selection of view angle

To explore the specific relationship between the view angle and the S/N of the light stripe images for a particular freeform prism, imaging experiments using a line laser sensor on one surface of the freeform prism are conducted in this paper. The experiments involved varying the angle between the incident light and the normal vector of the surface being tested, capturing light stripe images at view angles ranging from 0° to 40° , and then extracting the positions of the light stripes to analyze the S/N of the images. Figure 2 illustrates the original images captured by the CCD when the view angles are 0° , 10° , 20° , 30° , and 40° , along with the position of the extracted light stripes and the distribution of their intensities. It can be seen that at a view angle of 30° , due to the structure of the sensor, the reflected light was directed toward the CCD, resulting in a significant glare spot in the image, severely affecting the extraction accuracy for the light stripes. As the view angle decreased or increased from the center angle of 30° , the glare spot gradually moved out of the measurement area, and the intensity of the light received by the CCD weakened until it significantly impacted the extraction of the light stripe. The experimental results indicate that the directional diffuse reflection distribution on the freeform prism surface is complex. Therefore, an appropriate measurement view angle is essential to capture the surface profile accurately.

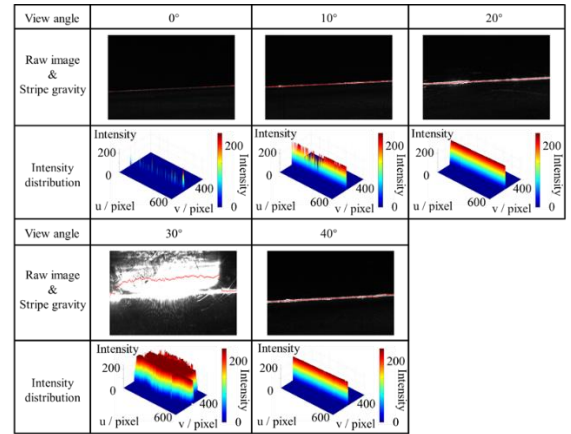


Fig. 2 Image, stripe gravity, and intensity distribution change with view angle.

To guide the selection of the optimal view angle, this paper proposed an S/N evaluation method aimed at quantifying the quality of light stripes in images. Considering that the line laser sensor uses the gray center point method to extract the light stripe center, the following two evaluation metrics are selected based on the calculation principles of this method:

The gray-scale criterion I_L : The brightness of the light stripe should be strong enough; otherwise, it will affect the extraction of the light stripe centroid, leading to noise in the measurement results. To avoid generating noise points, we set the gray-scale criterion I_L . Only when the pixel gray-scale intensity is above the set criterion is it included in the light stripe extraction calculation.

The width criteria K_L and K_H : The width of the light stripe should fall within a reasonable range. Overly wide light stripes are mainly caused by overexposure, while overly narrow ones are mainly caused

by stray light. To avoid introducing noise points from overexposure and stray light, we set the width criteria K_L and K_H . When the number of pixels in a column that meets the gray-scale criterion I_L is more than K_H or less than K_L , that column is recorded as noise; otherwise, it is recorded as a signal.

Combining the above two criteria, assume that the image has M columns, and the number of pixels in each column with a light intensity greater than I_L is K_i , $i=1\cdots M$, with the light intensity being I_k , $k=1\cdots K_i$. Then, for any column in the image, the signal intensity I_{Si} and noise intensity I_{Ni} can be calculated by Equations (2) and (3), respectively:

$$I_{Si} = \begin{cases} \sum_{k=1}^{K_i} I_k & K_L \leq K_i \leq K_H \\ 0 & K_i < K_L \text{ or } K_i > K_H \end{cases} \quad (2)$$

$$I_{Ni} = \begin{cases} 0 & K_L \leq K_i \leq K_H \\ \sum_{k=1}^{K_i} I_k & K_i < K_L \text{ or } K_i > K_H \end{cases} \quad (3)$$

For the entire image, the S/N ratio of the light stripe can be calculated using the following formula:

$$S/N = 10 \lg \left(\frac{\sum_{i=1}^M I_{Si}}{\sum_{i=1}^M I_{Ni}} \right) \quad (4)$$

Based on the light above stripe S/N evaluation method, we calculated the S/N of the light stripe at each view angle in 1° increments. By fitting these values with a spline curve, we plotted the curve of the light stripe S/N as a function of the view angle, as shown in Figure 3. As the view angle gradually increases from 0° , the intensity of the light stripes progressively rises, resulting in a gradual increase in the S/N. Upon reaching 28.2° , the S/N of the light stripe peaks at a local maximum value. Subsequently, with the ingress of specular reflection light into the CCD, although the intensity of the light stripe continues to rise, the intensity of stray light escalates rapidly. Through analysis of the S/N variation curve, it can be inferred that the optimal measurement effect of this system on this surface is achieved when the view angle is 28.2° . This angle will be a prerequisite for the path calculation. It's worth noting that for freeform prisms, the optical characteristics of different test surfaces may vary. Therefore, the experiment above must be replicated to determine the optimal view angles for measuring other surfaces.

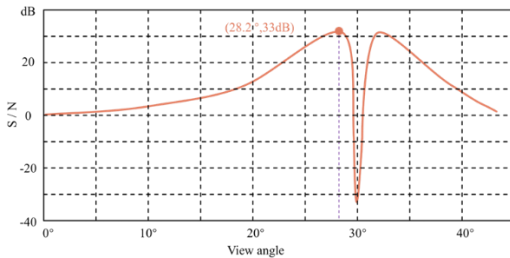


Fig. 3 S/N of the light stripe of the image changes with the view angle.

2.3. Iterative measurement procedure of the part

Due to factors such as manufacturing and assembly errors, the posture of the workpiece in the measurement coordinate system may deviate from its design posture. This deviation can cause the

measurement path generated based on the fixture assembly relationship to fail to accurately conform to the surface of the workpiece, resulting in incomplete measurement data.

The part posture iteration strategy proposed in this paper is illustrated in Figure 4. By utilizing biased paths for actual part measurement, incomplete measurement results are obtained. Point cloud registration is then employed to match the model point cloud to the posture of the measurement results. This alignment procedure ensures that the registered model point cloud closely matches the actual posture, thus enabling the calculation of a more accurate measurement path using the registered point cloud. The measurement and registration procedure are then repeated iteratively. As the iteration progresses, the model posture gradually converges toward the actual posture, resulting in an increasingly accurate measurement path and more complete measurement results. This iterative refinement continues until the measurement results no longer expand. At this point, the model posture is considered the actual posture of the part.

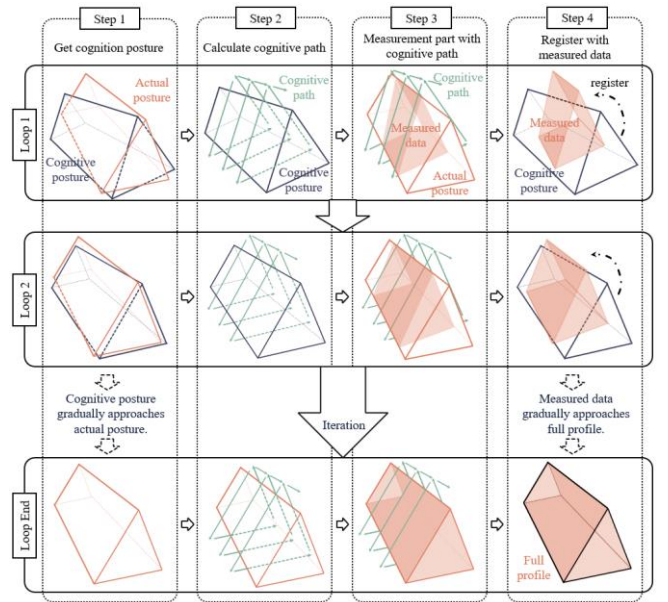


Fig. 4 Iterative measurement procedure.

3. Experimental results and discussion

This paper measured the surface morphology of a free surface prism, as shown in Figure 5 (a). This prism has three freeform surfaces that need to be measured, with a large spatial size and the area to be measured. The external cube size is approximately $80 \text{ mm} \times 50 \text{ mm} \times 30 \text{ mm}$. At the same time, its surface normal vector points in various directions in space, as shown in Figure 5 (b). By distributing its surface normal vector onto the unit sphere, as shown in Figure 5 (c), it can be seen that it is distributed in three regions in space, with significant differences between each region. The size and structure of this freeform surface prism have the general characteristics of polyhedral optical parts and can represent the measurement difficulties of most polyhedral optical parts.

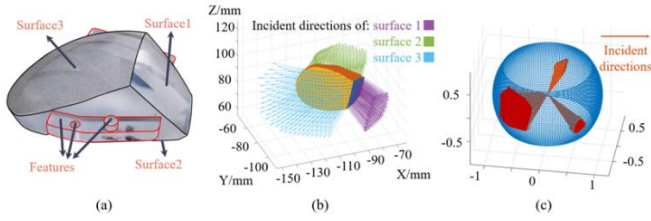


Fig. 5 Distribution of the normal vector of the freeform prism. (a) Physical diagram of polyhedral freeform surface prism. (b) Normal vector of the prism. (c) Distribution on the unit sphere of the normal vector.

The initial posture of the workpiece was determined based on the fixture design dimensions. The contours of the central region of each prism face were used for angle selection. The coordinates and normal vectors of the midpoints of each contour line in the world coordinate system were obtained from the initial posture. According to the content of Section 2.2, the movements of each axis for measuring the selected contour line from different observation angles were calculated to obtain the optimal view angle.

Then, the iterative measurement experiments were conducted, as shown in Figure 6. The model point cloud was matched to the measurement data posture, yielding new cognitive postures, calculating new cognitive measurement paths, and repeating this procedure to complete the measurement area gradually. As the iterative measurement procedure progressed, the measurement ranges of each surface gradually expanded, and the positions of the edges with significant curvature changes on the surface gradually became fully measured. The final measured area accounted for 99.35% of the prism surface, indicating the completion of full-profile measurement of the polyhedral freeform surface prism. The entire measurement process involved three iterative measurements, with each scan taking approximately 4 minutes and the total measurement process lasting around 15 minutes. The process is highly automated and requires no manual intervention. Figure 7 displays the measurement results of each surface, which are matched with the given model separately. The PV values of errors for each surface were $19.6\text{ }\mu\text{m}$, $23.4\text{ }\mu\text{m}$, and $18.9\text{ }\mu\text{m}$, consistent with their machining accuracy, indicating high measurement accuracy for individual surfaces of the prism.

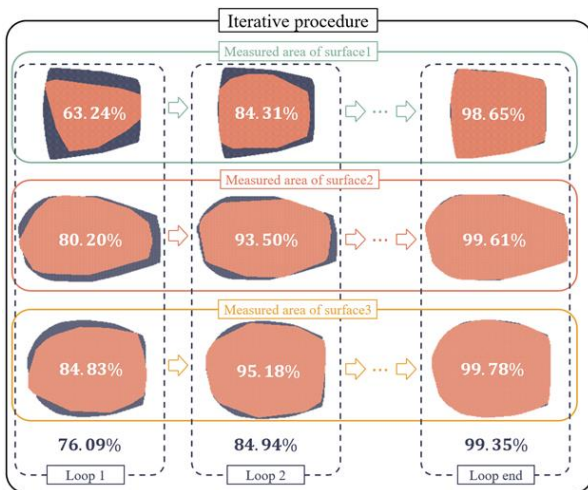


Fig. 6 Changes in measurement area during the iterative measurement

procedure.

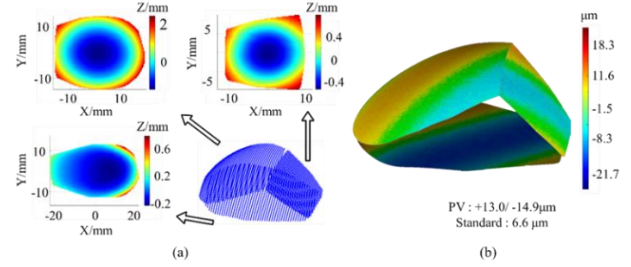


Fig. 7 Results of full-profile measurement and overall matching error. (a) Full-profile measurement result. (b) Matching error of measurement result.

3. Conclusions

This paper focuses on the problem of view angle selection and path accuracy in measuring the full profile of polyhedral freeform surface prisms using a line laser. Our conclusions are as follows: (1) A scanning measurement system based on a line laser and five axes is constructed. (2) A method for calculating the S/N of image stripes is proposed, and the optimal view angle of the measurement surface is selected based on the S/N to achieve the best imaging performance. (3) An iterative measurement method is proposed, which enables the automatic optimization of the measurement path, thereby achieving a complete full-profile measurement of freeform triangular prisms.

ACKNOWLEDGEMENT

This work is supported by National Natural Science Foundation of China (62373274).

REFERENCES

1. D. Cheng, H. Chen, C. Yao, Q. Hou, W. Hou, L. Wei, T. Yang, Y. Wang, Cheng D, Chen H, Yao C, et al. Design, stray light analysis, and fabrication of a compact head-mounted display using freeform prisms[J]. Optics Express, 2022, 30(20): 36931-36948.
2. J. Yu, Z. Shen, Z. Wang, Yu J, Shen Z, Wang Z. Compact dual band/dual FOV infrared imaging system with freeform prism[J]. Optics Letters, 2021, 46(4): 829-832.
3. Z. Liu, S. Wu, Q. Wu, C. Quan, Y. Ren, Liu Z, Wu S, Wu Q, et al. A novel stereo vision measurement system using both line scan camera and frame camera[J]. IEEE Transactions on Instrumentation and Measurement, 2018, 68(10): 3563-3575.
4. He X D, Torrance K E, Sillion F X, et al. A comprehensive physical model for light reflection[J]. ACM SIGGRAPH computer graphics, 1991, 25(4): 175-186.